

PAPER • OPEN ACCESS

## Convergence of SART + OS + TV iterative reconstruction algorithm for optical CT imaging of gel dosimeters

To cite this article: Yi Du *et al* 2017 *J. Phys.: Conf. Ser.* **847** 012025

View the [article online](#) for updates and enhancements.

### Related content

- [Computational simulations of the influence of angular rotation deviations in optical CT imaging of gel dosimeters](#)  
Yi Du, Gongyi Yu, Xincheng Xiang et al.
- [Computational simulations of the influence of background noise removal in optical-CT imaging of gel dosimeters](#)  
Yi Du, Gongyi Yu, Xincheng Xiang et al.
- [Influence of Iterative Reconstruction Algorithms on PET Image Resolution](#)  
G E Karpetas, C M Michail, G P Fountos et al.

# Convergence of SART + OS + TV iterative reconstruction algorithm for optical CT imaging of gel dosimeters

Yi Du<sup>1,2</sup>, Gongyi Yu<sup>1,3</sup>, Xincheng Xiang<sup>1</sup>, Xiangang Wang<sup>1</sup>, Yves De Deene<sup>2</sup>

<sup>1</sup>Institute of Nuclear and New Energy Technology, Tsinghua University, Beijing, 100084, China

<sup>2</sup>The Biomedical Engineering Laboratory, Department of Engineering, Macquarie University, Sydney, 2109, Australia

<sup>3</sup>Department of Radiation Oncology, Fudan University Shanghai Cancer Center, Shanghai, 200032, China

E-mail: wangxiangang@tsinghua.edu.cn

**Abstract.** Computational simulations are used to investigate the convergence of a hybrid iterative algorithm for optical CT reconstruction, i.e. the simultaneous algebraic reconstruction technique (SART) integrated with ordered subsets (OS) iteration and total variation (TV) minimization regularization, or SART+OS+TV for short. The influence of parameter selection to reach convergence, spatial dose gradient integrity, MTF and convergent speed are discussed. It's shown that the results of SART+OS+TV algorithm converge to the true values without significant bias, and MTF and convergent speed are affected by different parameter sets used for iterative calculation. In conclusion, the performance of the SART+OS+TV depends on parameter selection, which also implies that careful parameter tuning work is required and necessary for proper spatial performance and fast convergence.

## 1. Introduction

Gel dosimetry has received growing research interest for its outstanding three-dimensional dose measurement performance [1]. Upon irradiation, the radio-sensitive chemicals in gel dosimeters will react to the localized absorbed dose, which then induces changes in physical properties, such as relaxation time and optical density (OD). These changes can be read out by either MRI or optical CT, and, after calibration, three-dimensional dose maps can be obtained. Compared with MRI, optical CT has been proposed as an easily accessible and cost-efficient alternative for gel dosimeter readout [2-4].

In a typical optical CT scanning, optical transmission attenuated projections are captured by a detector, such as a photo-diode or CCD camera. When projections over 360 degrees are acquired, tomographic optical density images representing ODs can be reconstructed by either filtered backprojection (FBP for 2D, and FDK for 3D) or iterative algorithms. Subsequently, dose maps can be restored via dose-OD calibration. Optical CT traverse projections are often corrupted by noise and imperfection [5]. Compared with the filtered backprojection algorithm, iterative reconstruction has shown advantageous performance in noise and artefact suppression [6]. Based on our previous work, we have proposed a novel hybrid iterative optical CT reconstruction, i.e., simultaneous algebraic reconstruction technique (SART) integrated with ordered subsets (OS) iteration and total variance (TV) minimization regularization, i.e., *SART+OS+TV*. The method is detailed and fully evaluated in [7], which can be briefed as



$$f_j^{(k+1)} = f_j^{(k)} + \lambda \mathbf{R}^T \left( g_j^{(k)} - \frac{\mathbf{R}_{i,j} f_j^{(k)}}{\|\mathbf{R}\|_2} \right) \quad (1)$$

$$\min[TV(f_j^{(k)})] = \min \left[ \int_x \int_y \sqrt{\left( \frac{\partial f_j^{(k)}}{\partial x} \right)^2 + \left( \frac{\partial f_j^{(k)}}{\partial y} \right)^2} dx dy \right] \quad (2)$$

where  $f$  is the tomographic image to reconstruct,  $g$  is the logarithmic projections,  $\lambda$  is a relaxation factor, and  $\mathbf{R}$  is the system matrix (or projection operator) for optical transmission imaging geometry and physics;  $k$  stands for the  $k$ th ordered subset of projections, and  $j$  for the  $j$ th beamlet. In (1), we calculate the deviations between acquired projections and *reprojected* projections from the OD image  $f$  by forward projection, and use the projection deviations as error feedback to update the image by backprojection. In (2), the TV of OD image  $f$  is decreased iteratively to suppress noise and artefacts. In numerical implementation of this algorithm, three key parameters need to be chosen, which are the relaxation factor  $\lambda$  in (1) for SART iteration, the number of subsets  $N$  for OS iteration, and the relaxation factor  $\alpha$  in primal-dual algorithm for TV minimization [8]. The details and evaluation of this hybrid algorithm for optical CT imaging is under draft for comprehensive discussion. In conclusion, this algorithm outperforms classical FDK in denoising, edge-preserving and artefact reduction.

As a significant but relatively independent section of the work on SART+OS+TV algorithm, the convergence of this hybrid algorithm is discussed using computational simulations.

## 2. Methods and Materials

### 2.1. Simulation Setup

#### 2.1.1. Synthetic Phantom

A synthetic phantom is used for optical CT imaging simulation, which facilitates us to observe the iterative reconstruction process. The synthetic phantom is derived from [9] to mimic dose distribution in tissue equivalent gel irradiated by a 6-MV linac with 100cm SSD. The cylindrical phantom is 10 cm in diameter, and 10 cm in height, with a 2-cm wide square OD (irradiation) field offset 2-cm from the circular centre, as illustrated in Figure 1(a).

#### 2.1.2. Scenarios

The geometric parameters used in optical CT imaging correspond to the specifications of our optical CT scanner [10]. In order to observe the influence of parameter selection, we launched a series of scenarios with as many as 36 different parameter sets of the relaxation factor  $\lambda$ , the number of subsets  $N$  in OS, the relaxation factor  $\alpha$  in primal-dual algorithm for TV minimization. Compared with FDK, iterative reconstruction is time consuming. In this study, the calculation will be terminated once the iteration times reach 80.

### 2.2. Evaluation Metrics

The profiles of reconstructed images are given to see any bias from true OD values and dose gradient integrity performance. In the meantime, in order to describe the iterative convergence quantitatively, we choose the root-mean-square error (RMSE) for evaluation, which is defined as

$$RMSE^{(k)} = \sqrt{\frac{\sum_{i=1}^M (f_i^{(k)} - \hat{f}_i)^2}{M}} \quad (3)$$

where  $i$  is the  $i$ th pixel index in the image, and  $M$  is the total number of image pixels;  $f^{(k)}$  is the reconstructed image at the  $k$ th iteration, and  $\hat{f}$  is the true OD value of the phantom.

Meanwhile, since the synthetic phantom is cylindrical, we adopt the method in [11] to calculate the modulation transfer function (MTF) to describe the spatial resolution performance.

**Table 1.** Parameter sets for iterative reconstruction (IR).

Parameter Set No.	Parameter Item		
	$\lambda$	N	$\alpha$
# 1	0.001	12	0.0001
# 2	0.005	12	0.0001
# 3	0.001	4	0.0001
# 4	0.001	360	0.0005

**Table 2.** RMSEs of different methods.

Method	RMSE
FDK(Hann)	0.0054
FDK(RL)	0.0049
IR # 1	0.0050
IR # 2	0.0021
IR # 3	0.0059
IR # 4	0.0044

### 3. Results and Discussion

Four different sets of reconstruction parameter sets are given in Table 1 for this study. Comparison of the results reconstructed with different parameter sets show that the convergence is influenced by parameter selection. The RMSE is calculated as a metric for a central place inside the phantom region. As reference, the results of FDK with Hann and RL filters respectively are shown as well.

#### 3.1. Final Convergent Value

The profiles across the OD field of the synthetic phantom for different methods are plotted in Figure 1(b), and the RMSE results are given in Table 2. The small difference from the true ODs in both profiles and RMSEs implies that the results of the iterative method converge to true values without any significant bias.

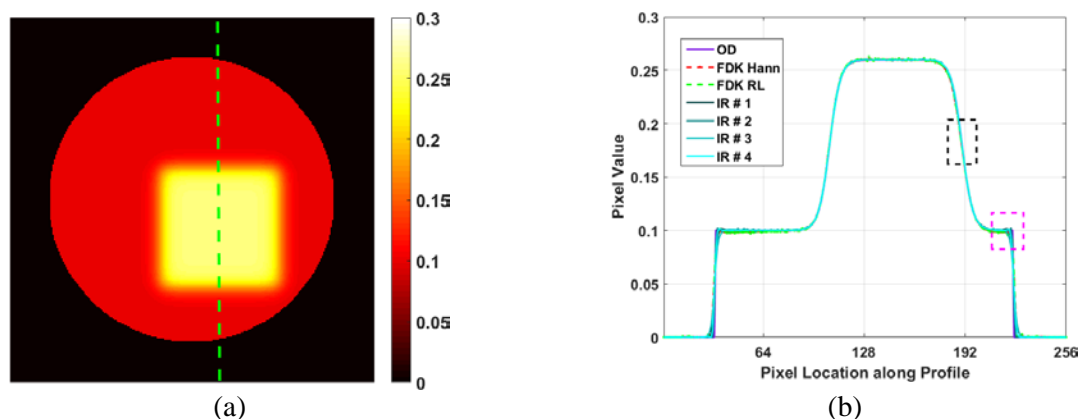


**Figure 1.** Synthetic Phantom profiles(a) and profiles of convergent results of different parameter sets with FDK as reference (b).

#### 3.2. Spatial Dose Gradient and Sharp Edge Integrity

Spatial dose gradients are important information for radiotherapy dosimetry, and the dose gradient integrity should be well preserved. In order to show the different performance in spatial gradient integrity, we selected a ROI inside the beam penumbra, and used the local profiles inside the ROI window for illustration. The ROI window we used is blue marked in Figure 1(b), and the profiles for different method are plotted in Figure 2(a).

Besides, in order to show the difference in spatial resolution, we used the circular edge of the synthetic phantom (in Figure 2(b)) for MTF calculation, the results of which are given in Figure 2(c). Comparing the dose gradients, edge profiles and MTF curves in Figure 2, we can see that in some case the results are smoother than that of FDK with a Hann filter, and in other case are sharper than FDK

with a RL filter. The variable ability in edge response and MTF implies that the SART+OS+TV algorithm is quite versatile in spatial gradient integrity and spatial resolution, which depends on parameter selection.

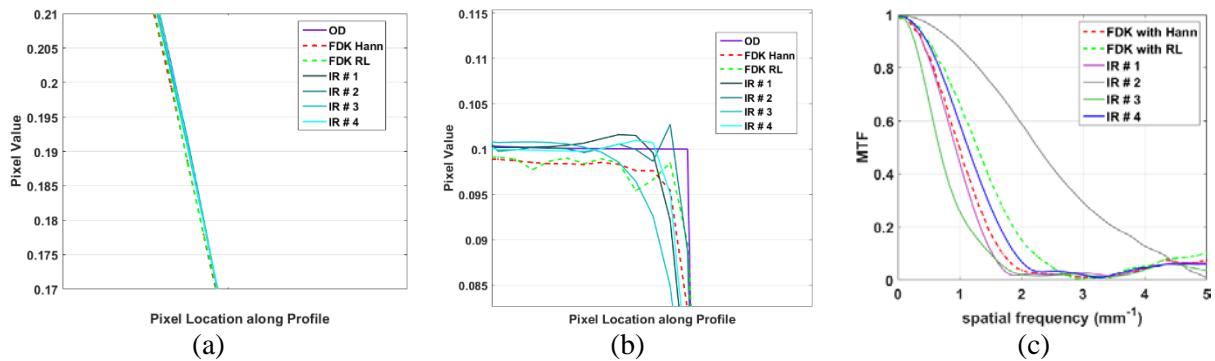


**Figure 2.** (a) Dose gradients of the blue ROI in Figure 1(b); (b) edge profiles corresponding to the pink ROI in Figure 1(b); (c) MTFs of different parameters with FDK as reference.

### 3.3. Rate of Convergence

The rate of convergence is a crucial characteristic in iterative reconstruction, which affects the computation cost. The MTF was calculated for different steps at intervals of 10 iterations to evaluate convergence. The MTF curves for different iterations and different sets of parameters are plotted in Figure 3. A clear difference in rate of convergence can be clearly observed for parameters.

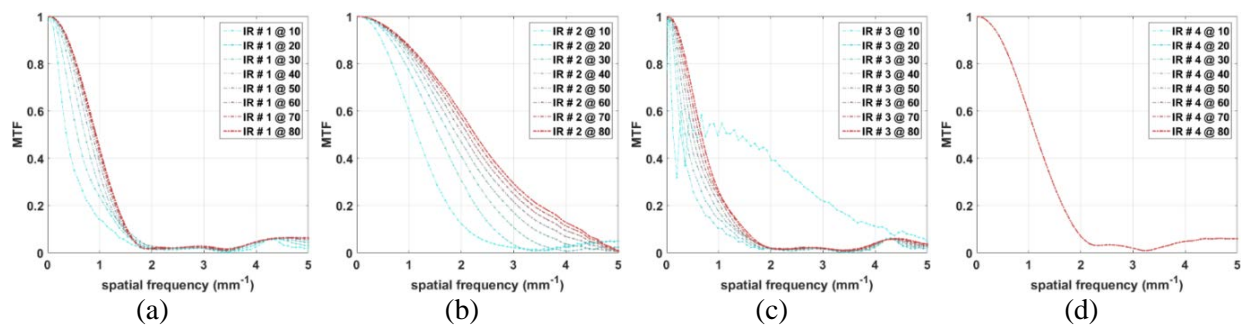


**Figure 3.** MTF curve clusters of parameter set #1(a), #2(b), #3(c), and #4(d). Note that in (d) the MTFs for iterations 10-70 superpose each other for fast convergence.

## 4. Conclusions

For the SART+OS+TV algorithm, a clear dependence of the rate of convergence on the parameter set is observed. The comparative analysis shows that the results converge to the true values without significant bias, and MTF and rate of convergence are affected by different combinations of parameters used for iterative calculation. In conclusion, careful parameter tuning is necessary for proper spatial performance and fast convergence with SART+OS+TV iterative reconstruction.

## 5. Acknowledgement

Jointly Supported by the National Science Foundation of China (No. 61571262, No.11575095, No. 61171115), and the National Key Research and Development Program (No. 2016YFC0105406).

## 6. References

- [1] Baldock C *et al* 2010 *Phys. Med. Biol.* **55** R1-63
- [2] De Deene Y *et al* 2002 *Phys. Med. Biol.* **47** 2459
- [3] De Deene Y and Baldock C 2002 *Phys. Med. Biol.* **47** 3117-41
- [4] De Deene Y *et al* 2002 *Phys. Med. Biol.* **47** 3441-63

- [5] Doran S J 2013 *J. Phys.: Conf. Ser.* **444** 012004
- [6] Yi D *et al* 2015 *J. Phys.: Conf. Ser.* **573** 012063
- [7] Du Y *et al* 2016 *Phys. Med. Biol.* **61** 8425-8439
- [8] Chambolle A and Pock T 2011 *J. Math. Imaging Vis.* **40** 120-45
- [9] De Deene Y 2015 *J. Phys.: Conf. Ser.* **573** 012076
- [10] De Deene Y 2015 *J. Phys.: Conf. Ser.* **573** 012058
- [11] Friedman S N *et al* W 2013 *Med. Phys.* **40** 051907